CO4-1 Development of Radiation Tolerant Image Sensor with Field Emitter Array

Y. Gotoh, M. Nagao[1], T. Okamoto[2], T. Masuzawa[3], Y. Neo[3], H. Mimura[3], H. Tsuji, M. Akiyoshi, I. Takagi, N. Sato[4]

Graduate School of Engineering, Kyoto University
[1]National Institute of Advanced Industrial Science and Technology
[2]National Institute of Technology, Kisarazu College
[3]Research Institute of Electronics, Shizuoka University
[4]Research Reactor Institute, Kyoto University

INTRODUCTION: One of the most serious problems for the observation of interior of the nuclear reactor at the Electric Power Plant, Fukushima the 1st, is such that there are no good cameras that can stand for the irradiation from radioactive material can be seen as a commercial product. Therefore, it is necessary to develop a reliable camera that can be used under hard radiation. The purpose of the present study is to develop a compact image sensor for visual light with a field emitter array (FEA). To ensure the radiation tolerance, it is necessary to show the resistance of each element against γ-ray radiation. Change in the operational characteristics of the key components of the image sensor, FEA [1] and photoconducting diode [2] was investigated.

EXPERIMENTS: The FEAs were fabricated at National Institute of Advanced Industrial Science and Technology. Photoconducting CdTe/CdS diodes were fabricated at National Institute of Technology, Kisarazu College. The irradiation of γ-rays to these devices was performed at Kyoto University Research Reactor Institute, Co-60 Gamma-ray Irradiation Facility. Irradiation of γ-ray to the FEAs was performed in a vacuum vessel made of glass. Current-voltage (*I-V*) characteristics of the FEA and CdTe/CdS photodiode were investigated before and after γ-ray irradiation. The dose of irradiation was between 60 and 200 kGy, depending upon the sample position during the irradiation.

RESULTS: Fig. 1 shows the *I-V* characteristics of the FEA in a triode configuration. No significant change of the *I-V* characteristics was observed even after the γ–ray irradiation with the dose of 125 kGy. Fig. 2 shows the *I-V* characteristics of the CdTe/CdS photodiode prepared on a graphite substrate (Substrate-type configuration). Also for this case, no significant change of the *I-V* characteristics was observed after the γ–ray irradiation with the dose of 75 kGy. Taking the fact that semiconductor image sensors have the life of 100 kGy, the FEA and the photoconducting CdTe/CdS diode have sufficient tolerance against γ–ray irradiation.

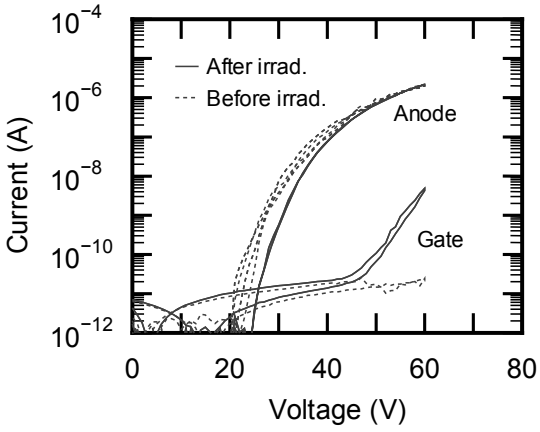

Fig. 1. *I-V* characteristics of FEA in triode configuration before and after γ-ray irradiation.

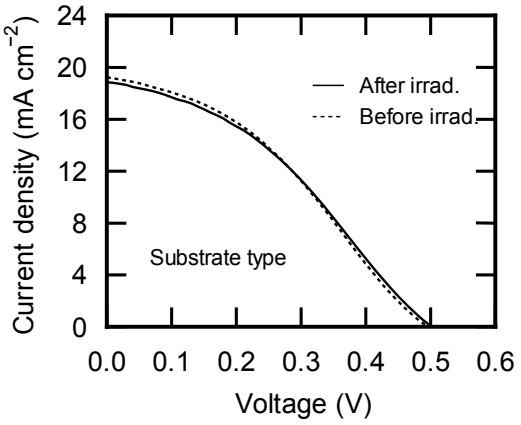

Fig. 2. *I-V* characteristics of CdTe/CdS diode in substrate-type configuration before and after γ–ray irradiation.

ACKNOWLEDGMENT: A part of this study is the result of "Development of radiation tolerant compact image sensor with a field emitter array", carried out under the Initiatives for Atomic Energy Basic and Generic Strategic Research by the Ministry of Education, Culture, Sports, Science and Technology of Japan.

REFERENCES:

[1] M. Nagao, Proc. of the 21st International Display Workshops, Dec. 3-5, 2015, Niigata (2015) 588-590.
[2] T. Okamaoto, R. Hayashi, S. Hara, Y. Ogawa, Jpn. J. Appl. Phys., **52** (2013) 102301/1-3.

採択課題番号 26002　耐放射線性に優れた微小真空冷陰極アレイ撮像素子の開　　通常採択
（京大院・工）後藤康仁、高木郁二、秋吉優史、辻　博司（静岡大・電研）根尾陽一郎
（京大・原子炉）佐藤信浩

CO4-2 Sub-Terahertz Absorption of Ionic Liquid

T. Awano and T. Takahashi[1]

Faculty of Engineering, Tohoku Gakuin University
[1]Research Reactor Institute, Kyoto University

INTRODUCTION: We have observed millimeter wave absorption bands around 6 and 8 cm^{-1} in AgI-superionic conductive glasses. These bands were also observed in CuI-superionic ones[1-3]. These bands seems to be due to collective motion of conductive ions, although how conduction ions moves in correlation is not clear.

Ionic liquid (IL) is molten salt at room temperature. It is interesting to compare ionic motion in ionic liquids with those in superionic conductor.

Recently, we have measured sub-terahertz absorption spectra of N,N-Diethyl-N-methyl-N-(2-methoxyethl) ammonium tetrafluoroborate ([DEME][BF_4]) and N,N-Diethyl-N-methyl-N-(2-methoxyethl)ammonium bis(trifluoromethanesulfonyl)imide ([DEME][TFSI]) [4]. Two absorption bands were observed around 6 and 8 cm^{-1}, which are almost coincident with those in AgI-superionic conductive glasses. These bands have almost equal peak positions and intensities in both ILs. This means that these absorption bands are due to cation motion. However, thermal change of these bands are different. This difference seems to be due to the difference of their phase transition temperatures and solid states. The former becomes glassy solid under 182 K. The latter becomes crystal.

To investigate these difference among ILs, measurements of absorption spectra of several ILs have been executed.

EXPERIMENTS: Ionic liquids (Tokyo Kasei. co., inc.) were spread into filter paper. Transmission spectra of single and double papers with ionic liquids were measured at room temperature and low temperatures. Absorption spectra were obtained by subtraction of them.

RESULTS: Fig. 1 shows absorption spectra of 1-Ethyl-3methylimidazolium tetrafluoroborate ([Emim][BF_4]). This ionic liquid becomes solid under 210 K. Fig. 2 shows absorption spectra of 1-Ethyl-3methylimidazolium bis(trifluoromethanesulfonyl)imide ([Emim][TFSI]) . Temperature dependence was different in these ionic liquids. The intensity of the absorption band of the former IL decreased gradually at temperatures above 227 K. On the other hand, that of the latter IL decreased rapidly at temperatures below 213 K. This difference seems to be due to the difference of their phase transition temperatures and glass or crystal structure of solid states of these ILs due to the anion difference.

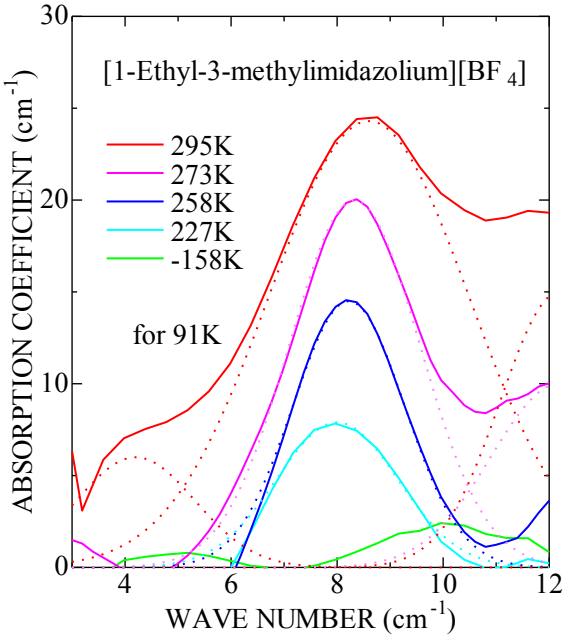

Fig. 1. Absorption increment spectra of [Emim][BF_4]. The baseline is the absorption spectrum at 91K.

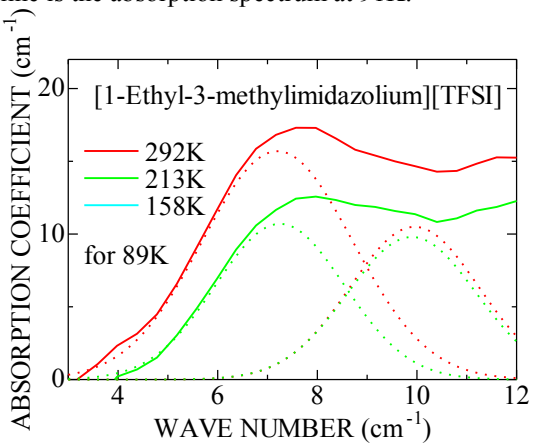

Fig. 2. Absorption increment spectra of [Emim][TFSI]. The baseline is the absorption spectrum at 89 K. The spectrum of 158 K was almost coincident with the baseline.

REFERENCES:

[1] T. Awano and T. Takahashi, J. Phys. Conf., **148** (2009) 012040/1-4.
[2] T. Awano and T. Takahashi, J. Phys. Soc. Jpn. **79** Suppl. A (2010) 118-121.
[3] T. Awano and T. Takahashi, Proceedings of the 13th Asian Conference on Solid State Ionics, (2012) 569-576.
[4] T. Awano and T. Takahashi, KURRI Progress Report 2013, CO4-5.

採択課題番号 26015 超イオン導電体におけるコヒーレントミリ波誘起イオン伝導の検証 通常採択
（東北学院大・工）淡野照義、（京大・原子炉）高橋俊晴

CO4-3

Generation of Circular Polarization using Linearly Polarized Coherent Transition Radiation

T. Takahashi

Research Reactor Institute, Kyoto University

INTRODUCTION: In recent years various types of coherent radiation emitted from a short bunch of relativistic electrons have attracted a considerable attention as a bright light source in the THz-wave and millimeter wave regions for the spectroscopic purpose. Coherent transition radiation (CTR), which is emitted from a boundary between two media, is one of such a coherent light source. CTR is usually utilized as a non-polarized light source, because the electric vector of transition radiation (TR) emitted from a metallic screen is axially symmetric with respect to the trajectory of an electron beam. In my previous reports [1, 2] the property of CTR emitted from a pair of wire-grid radiators with the different polarization was experimentally investigated in order to develop a new technique of generation of circular polarized THz radiation. Circularly polarized light has been useful in the circular dichroism spectroscopy. Shibata *et al*. has developed a technique of generation of circularly polarized millimeter-wave radiation with the phase difference between the forward TR and the backward one [3]. However, it was difficult to control the polarization degree in that technique. In this report circularly polarized CTR has been generated with a new technique. With this technique the polarization degree is able to be controlled precisely.

EXPERIMENTAL PROCEDURES: The experiment was performed at the coherent radiation beamline [4] at the L-band linac of the Research Reactor Institute, Kyoto University. The energy, the width of the macro pulse, and the repetition rate of the electron beam were 42 MeV, 33 ns, and 20 Hz, respectively. The average current of the electron beam was 0.5 μA. Two wire-grid polarizers (WG1 and WG2) 10 μm thick with 25 μm spacing were used in order to generate the CTR with horizontal and vertical components, respectively. Each CTR was superposed with phase difference through the optical delay system. Although a Martin-Puplett-type interferometer is usually used as a spectrometer, a grating-type monochromator was used in this experiment. The monochromator was set for the wavelength of 2.3 mm. The CTR was detected by a liquid-helium-cooled Si bolometer. In order to analyze the polarization degree a wire-grid polarizer with a rotary holder was used in front of the detector.

RESULTS: The observed polarization diagrams of CTRs from WG1 (horizontal component) and WG2 (vertical component) are shown in Fig.1 and 2, respectively. In these figures the degrees 0 and 180 represent the vertical plane, and 90 and 270 represent the horizontal plane. These results demonstrate that CTR from the wire grid has perfect linear polarizations. The observed polarization diagram of the superposition of these two CTRs is shown in Fig.3. This figure represents that the circular polarized CTR was generated.

REFERENCES:

[1] T. Takahashi, *et al.*, KURRI-PR 2012 CO4-15.
[2] T. Takahashi, *et al.*, KURRI-PR 2013 CO4-12.
[3] Y. Shibata *et al.*, Rev. Sci. Instrum. **72** (2001) 3221.
[4] T. Takahashi *et al.*, Rev. Sci. Instrum. **69** (1998) 3770.

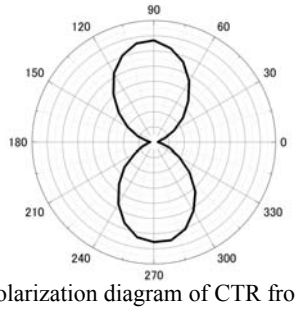

Fig.1. Polarization diagram of CTR from WG1.

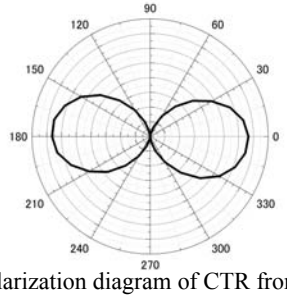

Fig.2. Polarization diagram of CTR from WG2.

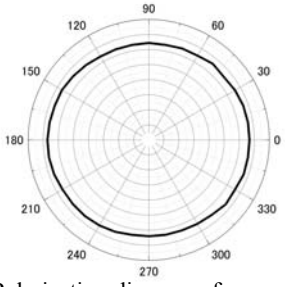

Fig.2. Polarization diagram of superposed CTR from WG1 and WG2.

採択課題番号 26016　コヒーレント遷移放射を用いたミリ波領域円偏光制御と近接場分光法に関する研究　　通常採択

（京大・原子炉）高橋俊晴、窪田卓見

CO4-4 Basic Study on Radiation-induced Luminescence from Natural Mineral

H. Fujita, M. Sakamoto[1], T. Saito[1]

Nuclear Fuel Cycle Engineering Laboratories, JAEA
[1]Research Reactor Institute, Kyoto University

INTRODUCTION: Dielectric materials such as natural minerals emit radiation induced luminescence such as thermoluminescence (TL) and optically stimulated luminescence (OSL). OSL is a well-established tool for measuring radiation doses in unfired sediments [1]. It has features in common with TL which has long been used in measuring radiation doses [2]. Both TL and OSL dosimetry with white mineral do not need to be specially installed in advance, prior to dose estimation. Quartz is an excellent material for use in dosimetry, because of its almost ubiquitous availability including an accidental place. Feldspar is an extensive ternary family of minerals appropriate for OSL and TL dosimetry as they display a strong luminescence and are quite common in the Earth's formation. However, the detailed emission mechanisms of TL and OSL from natural minerals such as natural quartz and feldspar are not yet clear. In this study, the emission mechanisms of TL and OSL were investigated in conjunction with various radiation-induced phenomena after annealing treatments of quartz samples, involving TL, OSL and electron spin resonance (ESR) measurements.

EXPERIMENTS: Two surface soil samples to 5 cm depth were collected at different places in Ibaraki. Natural quartz samples were extracted from the soils by a usual treatment of 6M hydrochloric acid (HCl), 6M sodium hydroxide (NaOH) followed by 60 min of concentrated hydrofluoric acid (HF). The etching treatment with HF solution was at room temperature. Further purification of the quartz grains was performed by hand selection for the sake of elimination of feldspar grains as low as possible. The purified quartz samples were sieved to adjust the grain sizes ranging from 150 μm to 250 μm in a diameter for ESR spectrometry, TL and OSL measurements. The quartz samples were annealed at 800 ºC for 24 hours in an electric furnace. The annealed quartz samples were irradiated a dose of 1 kGy with ^{60}Co source (0.73 kGy/h at D-30 cm) at room temperature at Kyoto University Research Reactor Institute (KURRI). The irradiated samples were stored at room temperature for one day to eliminate afterglow emission in dark room. The ESR measurement was carried out using an ESR spectrometer (Jeol Ltd., JES-TE 200) at −196 ºC. Prior to the ESR measurements, the quartz samples were annealed for 1 min at 50 ºC intervals ranging from 150 to 300 ºC as preheat treatment. Each remnant of the samples was kept in dark room without preheating treatment. After the ESR measurements, all luminescence measurements were performed using a JREC automated TL/OSL-reader system installed with a small X-ray irradiator (Varian, VF-50J tube). All preparations were carried out under dim red light.

RESULTS: In this research, the ESR signals of Al centers and Ti centers ($[TiO_4/H^+]^0$, $[TiO_4/Li^+]^0$ and $[TiO_4/Na^+]^0$) were detected in the annealed quartz samples. Al centers are hole-trapped centers and Ti centers are electron-trapped centers. Fig. 1 shows the intensity changes of the Al centers and the Ti centers. ESR signal intensity of Al centers decreased with preheating temperatures, gradually. On the other hand, ESR signal intensity of Ti centers showed different tendency from the ESR intensity of Al centers. The intensity of Ti centers increased or was constant up to 150 ºC of preheating temperature. After heating over 150 ºC, the intensity of Ti center decreased with preheating temperatures. The results agreed to our previous results. However, the intensity tendency of Ti centers was different between two quartz samples.

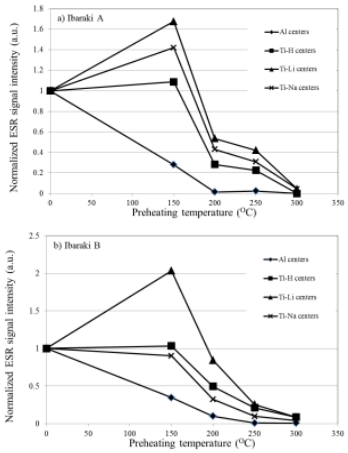

Fig.1 Tendency of ESR signal intensity with preheating temperature.

TL and OSL signals were measured using all kinds of quartz samples. However, their data was not evaluated, completely. Therefore, the data analysis will be conducted in 2015.

In this research, the luminescence emission mechanism could not be identified. Therefore, further work is necessary to identify luminescence mechanism using ESR measurement and annealing experiment.

REFERENCES:

[1] Huntley, D. J., et al., Nature 313, 105-107 (1985).
[2] Mckeever, S. W. S., Cambridge University Press, Cambridge, 103-105 (1985).

採択課題番号 26027　　天然鉱物からの放射線誘起ルミネッセンスの基礎的研究　　通常採択

（原子力機構、核サ研）藤田博喜（京大・原子炉）阪本雅昭、齊藤毅

CO4-5 Complex Structure of Ions Coordinated with Hydrophilic Polymer. 15. Applied Discussion with Ionic Behavior in Hydrophobic Matrixes.

A. Kawaguchi , Y. Morimoto

Research Reactor Institute, Kyoto University

INTRODUCTION: We have reported composite structure brought by *in situ* preparation through "secondary doping" by diffusion of metallic ions into iodine-doped hydrophilic polymers. Polyiodide ions, I_n^{m-} (*m, n*: integer, $n \neq 1$), which have been as solutes in aqueous solution, can be diffused into the polymers through immersing operation at room temperature. Or, the polymer matrix previously iodine-doped enhances following diffusion of other molecules or ions into matrix polymer; if the additional ion makes precipitates of inorganic salt with iodide, hybrid composite can be achieved without melting, nor casting, nor synthesizing.[1-3]

Such singularity suggests microscopic behavior of polymer chains as “pseudo solvents”, where ionic diffusion in nano-scale can be achieved or enhanced under affinity with polymer matrix keeping its structure: chain orientation, crystalline structure, self-organization,,etc. However, even if matrix is composed by “hydrophilic” polymers, their polarization or ionic affinity are not matched for ordinary hydrophilic solvents, such as water, ethanol,,etc.; hydrophilicity of polymeric matrixes should be much lower than that of hydrophilic low molecules, and that is a reason for general difficulty for charged ions to diffuse into the matrixes.

If so, observed rapid diffusion of polyiodides (“(1st) iodine doping”) or additional diffusion of metallic ions (“2nd doping”) should consistent with hydrophobicity of matrixes not only their hydrophilicity.[4,5] Then, similar procedures for “(1st) iodine doping” or “(2nd) Ag^+ ion doping” in hydrophobic matrixes were investigated as comparison with the previous results in hydrophilic matrixes.

EXPERIMENTS: Commercial "SEBS"-elastomer, AR-770C and AR-830C (Aron Kasei) were used as hydrophobic matrixes, which are composed of both polystyrene (hard segment) and polyethylene-polybutylene co-polymer (soft segment).

Iodine doping was achieved with I_2-KI(aq)/3.0N (for 22 hrs., at R.T.) and secondary doping was done with $AgNO_3$(aq)/0.25M (for 30min., at R.T.).

RESULTS: Present matrixes are just "hydrophobic" depending on their chemical components; generally, their activity to aqueous solution is so low that ionic diffusion or interaction should be negligible. However, ionic diffusion from aqueous solution into the hydrophobic matrixes was explicitly observed in coexistence of polyiodide ions. As shown in Fig. 1 and 2, “(1st) iodine doping” and “(2nd) Ag-doping” easily advanced into both *hydrophobic* matrixes in time of less than an hour at R.T. even with aqueous solvents. On the other hand, increase in mass (Δm, relative mass at each stage to non-doped sample) was much less than one for the previous hydrophilic matrixes: Δm less than 2%.

Furthermore, not only deep diffusion of polyiodide in “(1st) iodine doping” but “elution out” of polyiodide or Ag^+ ion in “(2nd) Ag-doping”.(Fig.1&2, right) Such behavior is analogous to “Stage III” which is observed in excessive “Ag-doping” to iodine-doped hydrophilic polymers.[6]

These results indicate that existence of polyiodide in polymeric materials can let ionic diffusion overcome general activation barrier.

ACKNOWLEDGEMENT: SEBS elastomers as hydrophobic samples, AR-770C and AR-830C, were presented by Aron Kasei Co.Ltd. The authors express great gratitude for them to inspire unexpected viewpoints.

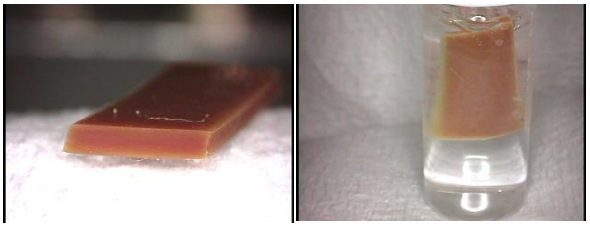

Fig. 1. AR-770C iodine-doped with I_2-KI(aq) (left) and following “(2nd) Ag-doping” with $AgNO_3$(aq) (right).

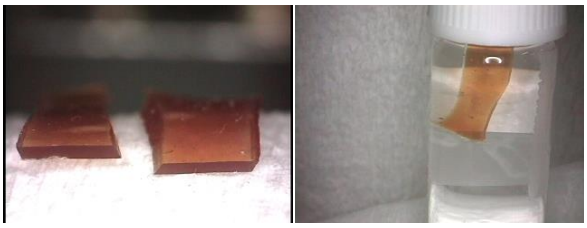

Fig. 2. AR-830C iodine-doped with I_2-KI(aq) (left) and following “(2nd) Ag-doping” with $AgNO_3$(aq) (right).

REFERENCES:

[1] A. Kawaguchi, Sens. Actuators B, **73** (2001) 174-178.

[2] Y. Gotoh, *et.al.*, Polym. Prep. Jpn., **51** (2002), 2259-2259.

[3] patent. JPN-5444559 (2014).

[4] KAWAGUCHI Akio, et.al., SPring-8 User Exp. Rep. **5** (2000A), 354-354. (2000)

[5] A. Kawaguchi, et.al., Macromol. Sym., **202**, 77-83. (2003)

[6] A. Kawaguchi, Polym. Prep. Jpn., **62**, 5116-5117. (2013)

採択課題番号 26052 親水性高分子ー金属塩ナノコンポジットの調製と構造 通常採択

（京大・原子炉）川口昭夫、森本幸生

CO4-6 Elucidation of Tritium Dynamics in Neutron Irradiated Tungsten

Y. Oya, M. Sato[1], K. Yuyama[1], T. Miyazawa[2], R. Okumura[3], Y. Iinuma[3], T. Fujii[3] and H. Yamana[3]

College of Science, Academic Institute, Shizuoka University
[1]Graduate School of Science, Shizuoka University
[2]Faculty of Science, Shizuoka University
[3]Research Reactor Institute, Kyoto University

INTRODUCTION: Tungsten (W) is a candidate material for the plasma facing components in the fusion future reactors due to the lower hydrogen isotopes retention. In a fusion reactor, W will be exposed to 14 MeV neutrons produced by the D-T fusion reaction during the plasma operation. Irradiation defects will be introduced by neutrons where hydrogen isotopes would be stably trapped, leading to the enhancement of fuel retention. Therefore, it is important to evaluate the hydrogen isotopes retention in neutron irradiated W. In this study, the deuterium retention behavior in neutron irradiated W was compared with that in heavy ion implanted W which has typical defects such as dislocation loops, vacancies and voids.

EXPERIMENTS: Disk type W (6 mm^{φ}×0.5 mm^{t}) purchased from A.L.M.T. Corp. Ltd was used as the sample. The samples were heat-treated at 1173 K under ultrahigh vacuum to remove the impurity and damages introduced by the polishing process. The neutron irradiation for the sample was performed at Pn-2 port in Kyoto University Research Reactor Institute (KUR) with the damage up to 4.3×10^{-4} dpa (displacement per atom). For the heavy ion irradiation, 6 MeV Fe^{2+} was irradiated into the samples at room temperature with the damage concentrations of 0.01 and 0.1 dpa by Takasaki Ion Accelerators for Advanced Radiation Application (TIARA) at Japan Atomic Energy Agency (JAEA). Thereafter, the samples were transferred to Shizuoka University for D_2^+ implantation. The samples were irradiated at R.T. with 1 keV D_2^+ with a flux of 8.75×10^{17} D m^{-2} s^{-1} to a fluence of 1.0×10^{22} D m^{-2}. The D desorption behavior was evaluated by thermal desorption spectroscopy (TDS) from room temperature up to 1173 K and 1273 K for Fe^{2+} irradiated samples and neutron-irradiated sample, respectively, with the heating rate of 0.5 K s^{-1}.

RESULTS: D_2 TDS spectra for various damaged W were shown in Fig. 1. The D desorption peaks consisted of four peaks at 400 K, 550 K, 650 K, 850 K corresponded to the adsorbed on the sample surface or trapped by dislocation loops, trapped by vacancies, vacancy clusters and voids [1-3]. No large difference for Peak 1 was found among 0.01 and 0.1 dpa Fe^{2+} irradiated samples, indicating that the retention of D adsorbed on the sample surface or trapped by dislocation loops would be almost saturated. However, for 0.1 dpa sample, major D desorption stage was shifted toward higher temperature side at 850 K, showing that voids would be more stable D trapping sites. In the case of fission neutron irradiation, only D retention as Peak 1 was increased, but its retention was almost the same as Fe^{2+} irradiated W, indicating that the dislocation loops for D trapping would be almost the saturation and no vacancy for D trapping was produced into the sample due to its lower damage concentration, or rhenium (Re) which produced by the transmutation caused by the thermal neutron irradiation, would contribute on the enhancement of D re-emission, although vacancies were produced. According to Ref. [4], due to the smaller size of Re atom than that of W atom, substitutional Re atom tends to bound to self-interstitial atoms (SIA) because their lattice strain field is opposite. Once the Re-SIA complex is formed, the mobility of the SIA decreases, leading to the enhancement of vacancy-interstitial recombination.

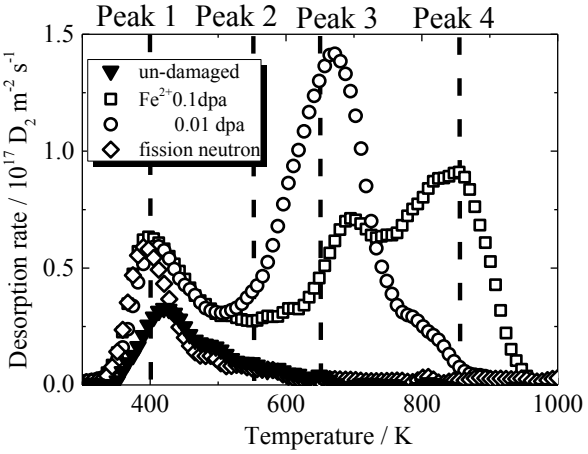

Fig. 1. D_2 TDS spectra for various damaged W.

REFERENCES:

[1] Eleveld H and Van Veen A *J. Nucl. Mater.* **191** (1992) 433-438.
[2] Iwakiri H et al., *J. Nucl Mater.* **307-311** (2002) 135-138.
[3] Luo G N et al., *Fusion Eng. Des.* **81** (2006) 957-962.
[4] Hasegawa A et al., *Fusion Eng. Des.* **89** (2014) 1568-1572.

採択課題番号 26063 中性子照射タングステンにおけるトリチウムダイナミックスの解明　通常採択（静大院・理）大矢恭久、佐藤美咲、湯山健太（静大・技術）宮澤俊義（京大・原子炉）奥村良、飯沼勇人、藤井俊行、山名元